

# Theoretical studies of the incommensurate magnetic structure of a heavy fermion system: $\text{CeRhIn}_5$

Torbjörn Björkman,<sup>1</sup> Raquel Lizárraga,<sup>2,3</sup> Fredrik Bultmark,<sup>1</sup> Olle Eriksson,<sup>1</sup> John M. Wills,<sup>3</sup> Anders Bergman,<sup>1</sup> Per H. Andersson,<sup>4</sup> and Lars Nordström<sup>1</sup>

<sup>1</sup>*Department of Physics and Astronomy, Ångström Laboratory, Uppsala University, P.O. Box 516, 751 20 Uppsala, Sweden*

<sup>2</sup>*Instituto de Física, Facultad de Ciencias, Universidad Austral de Chile, Casilla 567, Valdivia, Chile*

<sup>3</sup>*Theoretical Division, Los Alamos National Laboratory, Los Alamos, New Mexico 87545, USA*

<sup>4</sup>*Swedish Defence Research Agency (FOI), 164 90 Stockholm, Sweden*

(Received 9 October 2009; revised manuscript received 17 February 2010; published 26 March 2010)

We have investigated the electronic structure and the incommensurate magnetic configuration of the pressure-induced superconductor  $\text{CeRhIn}_5$ . Noncollinear first-principles calculations were performed in the local-density approximation plus  $U$  scheme. The observed magnetic configuration is described accurately in our calculations, especially considering the minute energy scale which is relevant (microelectron volt). The band structure and Fermi surfaces were investigated and nesting was found to be responsible for the complex noncollinear magnetic state of  $\text{CeRhIn}_5$ .

DOI: [10.1103/PhysRevB.81.094433](https://doi.org/10.1103/PhysRevB.81.094433)

PACS number(s): 75.30.Ds, 71.18.+y, 74.70.-b

## I. INTRODUCTION

$\text{CeRhIn}_5$  belongs to the family of heavy fermion superconductors in which superconductivity develops out of a normal state where electronic correlations produce a large enhancement of the effective mass of the conduction electrons. The temperature dependence of some physical properties below the superconducting transition temperature  $T_c$  in these metallic compounds is inconsistent with the well-established Bardeen-Cooper-Schrieffer (BCS) theory of superconductivity. A magnetically mediated theory of superconductivity has been proposed to explain such a behavior.<sup>1,2</sup> Mathur *et al.*<sup>2</sup> considered a magnetic model where charge carriers are bound together forming Cooper pairs by magnetic spin-spin interactions. Their results for  $\text{CePd}_2\text{Si}_2$  and  $\text{CeIn}_3$  suggest that magnetic interactions may indeed give rise to unconventional superconductivity.

$\text{CeRhIn}_5$  is an antiferromagnet<sup>3</sup> at ambient pressure with a Néel temperature of 3.8 K and it becomes a superconductor below  $T_c=2.1$  K when pressure is applied (1.65 GPa). This compound crystallizes in the tetragonal  $\text{HoCoGa}_5$ -type structure ( $P4/mmm$ ) displayed in Fig. 1, which is common to the ambient-pressure superconductors,  $\text{CeIrIn}_5$ ,<sup>4</sup>  $\text{CeCoIn}_5$ ,<sup>5</sup> and  $\text{PuCoGa}_5$ .<sup>6</sup> This quasi-two-dimensional structure seems to be favorable for heavy fermion superconductivity, in the same way as the  $\text{TiCr}_2\text{Si}_2$  type is often observed in the BCS conventional superconductors as well as in some of heavy fermion superconductors.

Neutron-diffraction studies performed on  $\text{CeRhIn}_5$  have revealed an incommensurate magnetic structure with wave vector  $\mathbf{q}=(\frac{1}{2}, \frac{1}{2}, q_z)$ , where  $q_z=0.297$  at ambient pressure.<sup>7</sup> At a small applied pressure of 1 GPa, the wave vector shifts to  $q_z \approx 0.4$ , and this state is stable until at least 1.7 GPa.<sup>8,9</sup> Neutron diffraction<sup>7</sup> also revealed a staggered moment of  $0.75(2)\mu_B$  per Ce ion<sup>10</sup> at 1.4 K (other reported values of the Ce moment are  $0.8\mu_B$  per Ce ion<sup>11</sup> and  $0.6\mu_B$  per Ce ion<sup>12</sup>). At high temperatures, Curie-Weiss behavior of magnetic susceptibility corresponding to  $2.5\mu_B/\text{Ce}$ ,<sup>11</sup> i.e., the free-ion value of the moment.

Within an  $ab$  plane (the easy plane), magnetic moments on the Ce ion form a simple nearest-neighbor antiferromagnet on a square lattice and they spiral transversally along the  $c$  axis. Coexistence of antiferromagnetism and superconductivity under pressure ( $P=1.75$  GPa) in  $\text{CeRhIn}_5$  was been reported,<sup>13</sup> and neutron-diffraction and electrical-resistivity studies<sup>14</sup> determined a broader range of pressures ( $0.9 \leq P \leq 1.75$  GPa) than previous accounts<sup>13</sup> in which long-range magnetic order and superconductivity exist simultaneously. More recently, several nuclear quadrupolar resonance (NQR) experiments have confirmed this coexistence.<sup>15–17</sup> Rusz *et al.*<sup>17</sup> performed first-principles calculations using both generalized gradient approximation plus

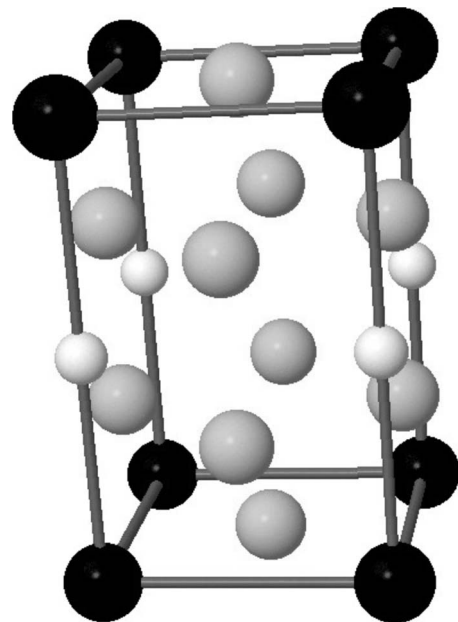


FIG. 1. The tetragonal crystal structure of  $\text{CeRhIn}_5$ . Ce and In ions are represented by black and light gray balls, respectively. The small balls correspond to Rh ions. The lattice parameters are  $a=4.65$  Å and  $c=7.54$  Å at 295 K.

$U$  and the so-called soft-core approximation and achieved a good description of  $\text{CeRhIn}_5$  when comparing to the NQR data. Fermi-surface measurements<sup>11</sup> and resistivity measurements<sup>18</sup> also indicate a localized state at ambient pressure going to a delocalized state at  $\sim 2.35$  GPa. In light of all these results, along with previous calculations,<sup>19</sup> it is clear that a model with a localized  $4f$  state should be correct at ambient pressure.

Our present investigation has been motivated by the complex noncollinear magnetic structure and the interesting relation between the relatively large ordered moments with unconventional superconductivity which in  $\text{CeRhIn}_5$  appears to be qualitatively different from other Ce-based heavy fermion superconductors. We performed noncollinear first-principles calculations using the full-potential augmented plane-wave method with local orbitals (FP-APW+lo).<sup>20,21</sup> This method allows us to study noncollinear magnetic structures such as the incommensurate structure in  $\text{CeRhIn}_5$ .<sup>7</sup> In this approach, the magnetization density is treated as a vector field free to vary in magnitude and direction everywhere. We studied different incommensurate structures described by the wave vector  $\mathbf{q}=(\frac{1}{2}, \frac{1}{2}, q_z)$  and the antiferromagnetic arrangement. Fermi-surfaces' nesting and the band structure of  $\text{CeRhIn}_5$  have also been investigated.

## II. CALCULATIONS

We have treated the  $4f$  state in Ce with the local-density approximation (LDA) plus  $U$  method using a double counting that interpolates between around mean field and the fully localized limit to minimize the total energy.<sup>22</sup> The  $U$  and the  $J$  parameters were taken from constrained LDA calculations of Anisimov and Gunnarsson<sup>23</sup> to be  $U=6$  eV and  $J=0.7$  eV. These values have previously been reported to describe localized Ce systems well.<sup>17,24</sup> We calculate total energies, band structure, and Fermi surfaces using the FP-APW+lo method<sup>20,21</sup> in a noncollinear implementation that allows us to treat spin spirals.<sup>25</sup> This scheme has been used to handle spin spirals in the rare earths<sup>26</sup> and rare-earth-based compounds<sup>27</sup> as well as in studies of the incommensurate magnetic structure of fcc Fe.<sup>21</sup> This approach relies on the introduction of the spin-spiral symmetries (symmetry operations with combined spin rotations and lattice translations) to restore the translational invariance of the magnetization density along the propagation direction. In this way, the chemical unit cell can be used instead of performing supercell calculations. However, it prevents us from including the spin-orbit coupling in the valence states since this interaction connects lattice and spin degrees of freedom. Therefore, if spin-orbit coupling is included in the calculation of the valence states, spin-spiral symmetries cannot be used.<sup>28</sup> Calculations were performed using the ELK code<sup>29</sup> at the lattice parameters obtained by previous paramagnetic FP linear muffin-tin orbitals (FP-LMTOs) calculations,<sup>30</sup>  $a=4.65$  Å and  $c=7.54$  Å which are in excellent agreement with experiments.<sup>31</sup> Brillouin-zone (BZ) integrations obtained by FP-APW+lo were performed using a  $k$ -point mesh  $8 \times 8 \times 32$ , together with a temperature broadening of  $k_B T=68$  meV. The size of the basis set was  $R_{\text{MT}} K_{\text{max}}=9$ ,

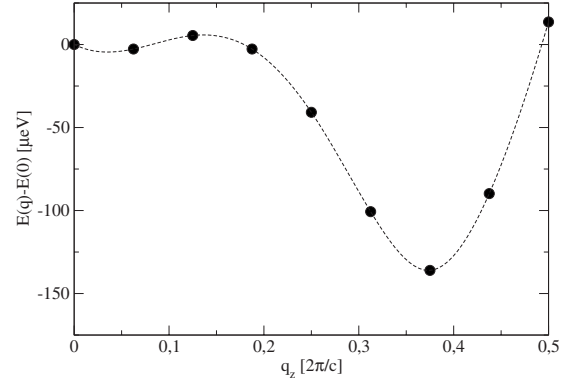


FIG. 2. The energy as function of the spin-spiral wave vector  $\mathbf{q}=(\frac{1}{2}, \frac{1}{2}, q_z)$ . The dashed line is a spline interpolation of the calculated points to guide the eyes.

where  $R_{\text{MT}}$  is the muffin-tin radius and  $K_{\text{max}}$  is the largest reciprocal-space wave vector.

## III. RESULTS

### A. Magnetism

The calculated spin magnetic moment of the Ce ion was found to be  $0.92\mu_B$  and the on-site moments for all other sites are very small, being the largest for Rh with a moment of  $0.006\mu_B$ . Since we cannot include spin-orbit coupling in the noncollinear scheme, the orbital moment is zero in our calculations.

Different spin spirals with wave vector  $\mathbf{q}=(\frac{1}{2}, \frac{1}{2}, q_z)$  were considered, including also the collinear configurations for  $q_z=0$  and  $q_z=\frac{1}{2}$ . The spin arrangement for  $q=0$  has a nearest-neighbors' antiferromagnetic coupling in the  $a$ - $b$  plane and a ferromagnetic interaction between the Ce layers. The total energy as a function of the wave vector  $\mathbf{q}=(\frac{1}{2}, \frac{1}{2}, q_z)$  was calculated and is shown in Fig. 2. Note that the energy scale is extremely small, which therefore sets a very high demand on the computational aspects of our study. Nevertheless, a distinct minimum appears at  $q_z=0.375$ , which means that the total energy is lowest for an incommensurate magnetic structure with a spin-spiral geometry.

In addition to the LDA+ $U$  calculations, we performed calculations in which the  $4f$  electron was treated as a core electron in the open-core approximation, using both FP-LAPW and tight-binding LMTO in the atomic sphere approximation. In neither of these approaches, could the spin spiral be stabilized, and this shows that the  $4f$  basis functions are essential to resolve the small energy differences involved in the spin-spiral calculation. We also performed LDA calculations, where the  $4f$  electron is treated as itinerant and this resulted in a nonmagnetic ground state, far from the experimental situation.

### B. Electronic structure

When discussing the electronic structure and its coupling to the magnetism, we first analyze the calculated density of states (DOS) of the valence band, which is shown in Fig. 3.

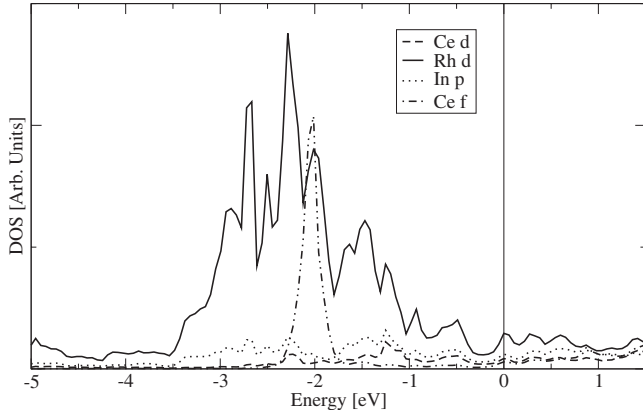


FIG. 3. Partial densities of states of CeRhIn<sub>5</sub> in the  $q_z=0$  configuration. The Fermi energy is at zero energy and is marked by a vertical line. The main contributions near the Fermi energy come from Ce  $d$ , Rh  $d$ , and In  $p$  states. The Ce  $f$  states contribute one electron and the sharp peak at  $-2$  eV. Only the majority-spin channel is shown and the minority is almost indistinguishable but lacks the Ce  $f$  peak.

The occupied part of the DOS is dominated by Rh  $d$  states that lie in the energy region between  $-4$  and  $-1.5$  eV. The main features of the Ce  $d$  states are located above the Fermi level. The Ce  $4f$  states are in our calculations found to be located at some 2 eV binding energy with very little spectral weight at the Fermi level whereas In  $p$  states form a rather uniform background to the DOS. We also notice in the figure that DOS at the Fermi level is very small.

The energy-band dispersion<sup>32</sup> along important symmetry lines in the BZ is depicted in Fig. 4, in a narrow energy interval around the Fermi level for a spin spiral with wave vector  $\mathbf{q}=(\frac{1}{2}, \frac{1}{2}, 0)$ . One may see in Fig. 4 that only few bands cross the Fermi level but the resulting Fermi surfaces are nevertheless rather complex, as shown in Fig. 5. Part of the complexity is caused by the shift of the energy bands imposed by the general symmetry of the wave function for spin-spiral geometries.<sup>28</sup> The surfaces are rather similar to the paramagnetic surfaces of Ref. 30 but here each figure contains two identical shapes, one corresponding to spin-up and the other to spin-down states. This is due to the antifer-

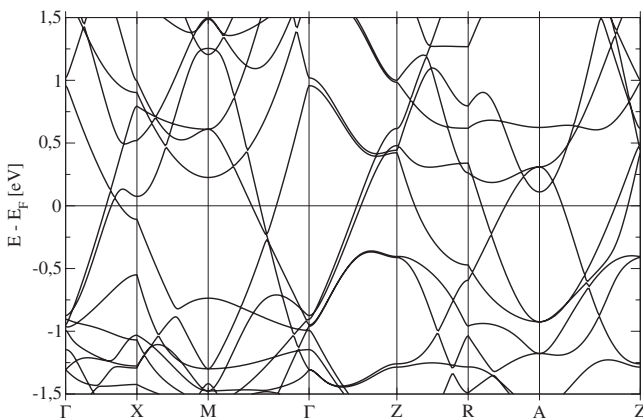


FIG. 4. Band structure for CeRhIn<sub>5</sub> with  $q=(\frac{1}{2}, \frac{1}{2}, 0)$ . The Fermi energy is shown by a horizontal dashed line.

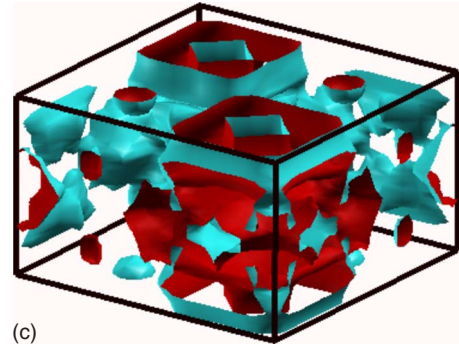
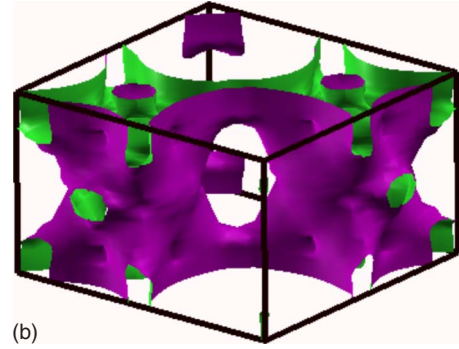
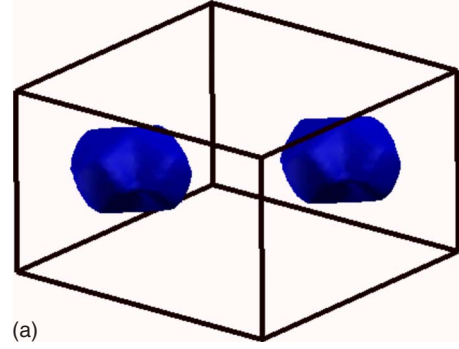


FIG. 5. (Color online) The first three Fermi-surface sheets of CeRhIn<sub>5</sub> in the antiferromagnetic  $\mathbf{q}=(\frac{1}{2}, \frac{1}{2}, 0)$  state in order of band index. The uppermost ball-shaped surface belong to the lowest band, the one in the middle is the second lowest and at the bottom is the highest band crossing the Fermi level. There is a fourth surface, not shown, which consists of a few very small scattered pockets.

romagnetic state in the  $xy$  plane. There is also a fourth sheet, not shown here, that consists of a few very small scattered pockets.

When analyzing the Fermi surfaces, it is of interest to investigate the nesting features between different Fermi-surface sheets. In earlier studies of magnetic structures of the rare-earth metals,<sup>26,33,34</sup> strong evidence of the existence of a relation between the wave vector  $\mathbf{q}$  of the magnetic structure and the Fermi-surface nesting, i.e., parallel portions of the Fermi surface separated by the wave vector  $\mathbf{q}$ , was observed. Since the generalized susceptibility becomes large for the  $\mathbf{q}$  that defines the nesting, a magnetic structure characterized by such a  $\mathbf{q}$  is expected to occur. Due to the complexity of the surfaces, we were unable to analyze the nesting by simple inspection so following Lizárraga *et al.*<sup>27</sup> we calculate

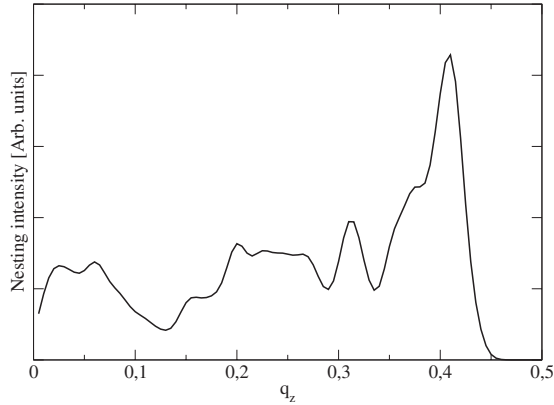


FIG. 6. Plot of the nesting intensity (see text) along the  $q_z$  direction for the Fermi surface calculated in the antiferromagnetic  $\mathbf{q}=(\frac{1}{2}, \frac{1}{2}, 0)$  state.

the nesting intensity of the surfaces along the  $q_z$  direction. This is a brute force analysis that is done by, for each piece of Fermi surface, counting the number of other pieces of surface that are encountered along some direction. Thus, we get a measure of the overlap of one sheet with itself or one of the other sheets, under translations along the  $q_z$  direction. Figure 6 shows our results where a clear peak around  $q_z = 0.4$  can be seen. This coincides with the calculated total-energy minimum in Fig. 2 for a spin spiral with  $q_z = 0.375$ . We therefore attribute the complex magnetic structure and the breaking of incommensurate symmetry of the spin spiral to Fermi-surface nesting. We also made attempts to identify if any parts of the surfaces were more “active” by mapping the nesting intensity onto the Fermi surfaces but no clear pattern emerged from this analysis.

#### IV. CONCLUSIONS

The electronic and magnetic structures of  $\text{CeRhIn}_5$  have been investigated by first-principles theory. A spin spiral with

wave vector  $\mathbf{q}=(\frac{1}{2}, \frac{1}{2}, 0.375)$  was found to be the ground-state magnetic configuration for the system. This is in fair agreement with the experimental finding of  $q_z = 0.298$  at ambient pressure and, given the small energy scale in these calculations (microelectron volt accuracy is needed), we believe the agreement with experimental findings is very good. The number found here is even closer to the value of  $q_z = 0.4$  reported for slightly elevated pressures (1 GPa) (Ref. 9) but since the whole of the interesting pressure range for the compound (0–4 GPa) is smaller than the pressure resolution for present electronic-structure schemes, it is hard to say exactly which of these two solutions our calculation describes. From analysis of the electronic structure, we have been able to identify the reason for the complex noncollinear magnetic structure of  $\text{CeRhIn}_5$  as Fermi-surface nesting.

Comparison of our calculated moments to experimental measurements is made difficult by the method of treating the spin spiral which forces us to neglect spin-orbit coupling. This approximation is not likely to affect the spin spiral since its driving force is the indirect exchange coupling of the localized spin moment to the valence band, and so the main concern of the theory is to get the correct spin moment. The calculated spin moments are close in magnitude to the total moments as observed in neutron-diffraction experiments<sup>7,11,12</sup> and from a crystal-field analysis.<sup>35</sup> This could indicate that the orbital moments are largely quenched in this material.

#### ACKNOWLEDGMENTS

Support from the Swedish Research Council (VR), STEM and the Swedish Foundation for Strategic Research (SSF) are acknowledged. We also acknowledge support from the Swedish National Super Computer facility (SNAC). We acknowledge valuable discussions with P. Oppeneer, F. Cricchio, and M. Colarieti-Tosti. R.L. would like to acknowledge support from FONDECYT Chile Project No. 11080259 and CONICYT Chile under Grant No. ACT24/2006.

<sup>1</sup>K. Miyake, S. Schmitt-Rink, and C. M. Varma, *Phys. Rev. B* **34**, 6554 (1986).

<sup>2</sup>N. D. Mathur, F. M. Grosche, S. R. Julian, I. R. Walker, D. M. Freye, R. K. W. Haselwimmer, and G. G. Lonzarich, *Nature (London)* **394**, 39 (1998).

<sup>3</sup>H. Hegger, C. Petrovic, E. G. Moshopoulou, M. F. Hundley, J. L. Sarrao, Z. Fisk, and J. D. Thompson, *Phys. Rev. Lett.* **84**, 4986 (2000).

<sup>4</sup>C. Petrovic, R. Movshovich, M. Jaime, C. Pagliuso, M. F. Hundley, J. L. Sarrao, Z. Fisk, and J. D. Thompson, *Europhys. Lett.* **53**, 354 (2001).

<sup>5</sup>C. Petrovic, C. Pagliuso, M. F. Hundley, R. Movshovich, J. L. Sarrao, J. D. Thompson, Z. Fisk, and P. Monthoux, *J. Phys.: Condens. Matter* **13**, L337 (2001).

<sup>6</sup>J. L. Sarrao, L. A. Morales, J. D. Thompson, B. L. Scott, G. R. Stewart, F. Wastin, J. Rebizant, P. Boulet, E. Colineau, and G. H. Lander, *Nature (London)* **420**, 297 (2002).

<sup>7</sup>W. Bao, P. G. Pagliuso, J. L. Sarrao, J. D. Thompson, Z. Fisk, J. W. Lynn, and R. W. Erwin, *Phys. Rev. B* **62**, R14621 (2000).

<sup>8</sup>S. Majumdar, G. Balakrishnan, M. R. Lees, D. McK. Paul, and G. J. McIntyre, *Phys. Rev. B* **66**, 212502 (2002).

<sup>9</sup>S. Raymond, G. Knebel, D. Aoki, and J. Flouquet, *Phys. Rev. B* **77**, 172502 (2008).

<sup>10</sup>W. Bao, P. G. Pagliuso, J. L. Sarrao, J. D. Thompson, Z. Fisk, J. W. Lynn, and R. W. Erwin, *Phys. Rev. B* **67**, 099903(E) (2003).

<sup>11</sup>R. Settai, T. Takeuchi, and Y. Ōnuki, *J. Phys. Soc. Jpn.* **76**, 051003 (2007).

<sup>12</sup>S. Raymond, E. Ressouche, G. Knebel, D. Aoki, and J. Flouquet, *J. Phys.: Condens. Matter* **19**, 242204 (2007).

<sup>13</sup>T. Mito, S. Kawasaki, Y. Kawasaki, G.-q. Zheng, Y. Kitaoka, D. Aoki, Y. Haga, and Y. Ōnuki, *Phys. Rev. Lett.* **90**, 077004 (2003).

<sup>14</sup>A. Llobet *et al.*, *Phys. Rev. B* **69**, 024403 (2004).

<sup>15</sup>S. Kawasaki *et al.*, *J. Phys. Chem. Solids* **67**, 497 (2006).

- <sup>16</sup>Y. Kohori, H. Taira, H. Fukazawa, T. Kohara, Y. Iwamoto, T. Matsumoto, and M. B. Maple, *J. Alloys Compd.* **408-412**, 51 (2006).
- <sup>17</sup>J. Ruzs *et al.*, *Phys. Rev. B* **77**, 245124 (2008).
- <sup>18</sup>G. Knebel, D. Aoki, J.-P. Brison, and J. Flouquet, *J. Phys. Soc. Jpn.* **77**, 114704 (2008).
- <sup>19</sup>S. Elgazzar, I. Opahle, R. Hayn, and P. M. Oppeneer, *Phys. Rev. B* **69**, 214510 (2004).
- <sup>20</sup>E. Sjöstedt, L. Nordström, and D. J. Singh, *Solid State Commun.* **114**, 15 (2000).
- <sup>21</sup>E. Sjöstedt and L. Nordström, *Phys. Rev. B* **66**, 014447 (2002).
- <sup>22</sup>A. G. Petukhov, I. I. Mazin, L. Chioncel, and A. I. Lichtenstein, *Phys. Rev. B* **67**, 153106 (2003).
- <sup>23</sup>V. I. Anisimov and O. Gunnarsson, *Phys. Rev. B* **43**, 7570 (1991).
- <sup>24</sup>A. B. Shick, W. E. Pickett, and A. I. Lichtenstein, *J. Electron Spectrosc. Relat. Phenom.* **114-116**, 753 (2001).
- <sup>25</sup>L. Nordström and D. J. Singh, *Phys. Rev. Lett.* **76**, 4420 (1996).
- <sup>26</sup>L. Nordström and A. Mavromaras, *Europhys. Lett.* **49**, 775 (2000).
- <sup>27</sup>R. Lizárraga, A. Bergman, T. Björkman, H.-P. Liu, Y. Andersson, T. Gustafsson, A. G. Kuchin, A. S. Ermolenko, L. Nordström, and O. Eriksson, *Phys. Rev. B* **74**, 094419 (2006).
- <sup>28</sup>L. Sandratskii, *Adv. Phys.* **47**, 91 (1998).
- <sup>29</sup><http://elk.sourceforge.net>, ELK is an open-source full-potential APW+lo code and was formerly called Exciting.
- <sup>30</sup>D. Hall *et al.*, *Phys. Rev. B* **64**, 064506 (2001).
- <sup>31</sup>E. G. Moshopoulou, Z. Fisk, J. L. Sarrao, and J. D. Thompson, *J. Solid State Chem.* **158**, 25 (2001).
- <sup>32</sup>The present calculated band structure for CeRhIn<sub>5</sub> and the results in the literature, e.g., Refs. [19](#) and [30](#) can be a little hard to compare since the bands are shifted in  $\mathbf{q}=(\frac{1}{2}, \frac{1}{2}, 0)$ . This shift comes from the representation of the wave function, the generalized Bloch spinors, that we have used in our study (see Ref. [36](#)).
- <sup>33</sup>S. C. Keeton and T. L. Loucks, *Phys. Rev.* **168**, 672 (1968).
- <sup>34</sup>A. R. Mackintosh, *Phys. Rev. Lett.* **9**, 90 (1962).
- <sup>35</sup>A. D. Christianson, J. M. Lawrence, P. G. Pagliuso, N. O. Moreno, J. L. Sarrao, J. D. Thompson, P. S. Riseborough, S. Kern, E. A. Goremychkin, and A. H. Lacerda, *Phys. Rev. B* **66**, 193102 (2002).
- <sup>36</sup>R. Lizárraga, S. Ronneteg, R. Berger, A. Bergman, O. Eriksson, and L. Nordström, *Phys. Rev. B* **70**, 024407 (2004).